How Epigallocatechin-3-gallate and Tetracycline Interact with the Josephin Domain of Ataxin-3 and Alter Its Aggregation Mode

ARTICLE *in* CHEMISTRY - A EUROPEAN JOURNAL · NOVEMBER 2015

Impact Factor: 5.73 · DOI: 10.1002/chem.201503086

ChemPubSoc Europe

DOI: 10.1002/chem.201503086

CHEMISTRY
A European Journal
Full Paper

Molecular Recognition

How Epigallocatechin-3-gallate and Tetracycline Interact with the Josephin Domain of Ataxin-3 and Alter Its Aggregation Mode

Marcella Bonanomi,[a] Cristina Visentin,[a] Antonino Natalello,[a, b, c] Michela Spinelli,[a, d] Marco Vanoni,[a, c, d] Cristina Airoldi,*[a, c, d] Maria E. Regonesi,*[a, c] and Paolo Tortora[a, c]

Abstract: Epigallocatechin-3-gallate (EGCG) and tetracycline are two known inhibitors of amyloid aggregation able to counteract the fibrillation of most of the proteins involved in neurodegenerative diseases. We have recently investigated their effect on ataxin-3 (AT3), the polyglutamine-containing protein responsible for spinocerebellar ataxia type 3. We previously showed that EGCG and tetracycline can contrast the aggregation process and toxicity of expanded AT3, although by different mechanisms. Here, we have performed further experiments by using the sole Josephin domain (JD) to further elucidate the mechanism of action of the two compounds. By protein solubility assays and FTIR spectroscopy we have first observed that EGCG and tetracycline affect the JD aggregation essentially in the same way displayed when acting on the full-length expanded AT3. Then, by saturation transfer difference (STD) NMR experiments, we have shown that EGCG binds both the monomeric and the oligomeric JD form, whereas tetracycline can only interact with the oligomeric one. Surface plasmon resonance (SPR) analysis has confirmed the capability of the sole EGCG to bind monomeric JD, although with a K_D value suggestive for a non-specific interaction. Our investigations provide new details on the JD interaction with EGCG and tetracycline, which could explain the different mechanisms by which the two compounds reduce the toxicity of AT3.

Introduction

Spinocerebellar ataxia type 3 (SCA3), also known as Machado–Joseph disease, is one among several polyglutamine (polyQ) diseases, autosomal dominantly inherited neurodegenerative disorders that also include Huntington's disease. They are caused by unstable expansions of $(CAG)_n$ trinucleotide-repeated sequences at disease-specific gene loci that are translated into elongated polyQ tracts.[1–3] Ataxin-3 (AT3) is the protein that triggers SCA3 when its polyQ stretch exceeds a critical length of about 55 consecutive residues.[4,5] AT3 consists of a globular N-terminal domain, the so-called Josephin domain (JD), and a flexible tail containing the polyQ tract.[6] By comparing different polyQ proteins, it appears that the protein context surrounding the polyQ tract can differently affect aggregation pathways and kinetics. In the case of AT3, extensive studies have focused on the intrinsic amyloidogenic properties of the JD, as well as on the role of the polyQ expansion on protein stability and aggregation kinetics.[7,8] It is known that the expansion of the polyQ tract beyond a critical threshold triggers misfolding and protein aggregation into sodium dodecyl sulfate (SDS)-insoluble amyloid fibrils.[9] Nevertheless, it has been demonstrated that the first step of the fibrillation is reversible, polyQ-independent, and proceeds through aggregation of the JD.[10,11]

Recently, we further characterized the aggregation intermediates of an expanded AT3 variant.[12] This is a prerequisite to correlate the protein structure with the toxicity and to determine the capability of specific compounds to counteract one or both steps of AT3 aggregation. In fact, by biochemical and biophysical approaches, we have recently demonstrated that epigallocatechin-3-gallate (EGCG) and tetracycline (Figure 1) can contrast the aggregation and toxicity of expanded AT3, although by different mechanisms.[13] EGCG is a polyphenolic flavonoid widely considered to be the key bioactive ingredient of green tea. It has been extensively studied, primarily for its beneficial effects, ranging from antitumor and anti-inflammatory properties to neuroprotective behavior. In fact, EGCG has been reported to affect multiple biological pathways, such as gene expression, growth-factor-mediated signaling, and antioxidant pathways.[14–16] Also, it is endowed with well-established metal-chelating properties.[17] However,

[a] Dr. M. Bonanomi,[+] C. Visentin,[+] Dr. A. Natalello, Dr. M. Spinelli, Prof. M. Vanoni, Dr. C. Airoldi, Dr. M. E. Regonesi, Prof. P. Tortora
Department of Biotechnology and Biosciences, University of Milano-Bicocca
Piazza della Scienza 2, 20126 Milano (Italy)
E-mail: cristina.airoldi@unimib.it
mariaelena.regonesi@unimib.it

[b] Dr. A. Natalello
Consorzio Nazionale Interuniversitario per le Scienze Fisiche della Materia (CNISM), UdR Milano-Bicocca, Milano (Italy)

[c] Dr. A. Natalello, Prof. M. Vanoni, Dr. C. Airoldi, Dr. M. E. Regonesi, Prof. P. Tortora
Milan Center of Neuroscience (NeuroMI), 20126 Milano (Italy)

[d] Dr. M. Spinelli, Prof. M. Vanoni, Dr. C. Airoldi
SysBio Centre for Systems Biology, Milano and Rome (Italy)

[+] These authors contributed equally to this work.

Supporting information for this article is available on the WWW under http://dx.doi.org/10.1002/chem.201503086.

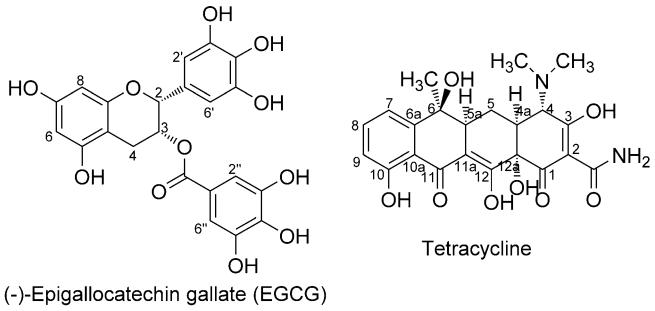

Figure 1. Structure and numbering of EGCG and tetracycline.

a wealth of data indicates that the antioxidant/metal-chelating capability of EGCG is unlikely to be the sole explanation for its neuro-rescue capacity. Plenty of works report on the capability of EGCG to interfere with the aggregation process of many amyloid proteins. It has been demonstrated that EGCG is able to inhibit the formation of toxic oligomers by steering misfolded Aβ,[18] α-synuclein,[19] transthyretin,[20] and mutant huntingtin[21] away from folding pathways that lead to amyloidogenic β-sheet-rich structures toward unstructured, non-toxic forms, either by binding the protein directly or possibly by acting as a protein chaperone. However, how EGCG works is not entirely clear. Its action seems to be largely independent of the primary sequence of the protein, given its capability to bind to unfolded bovine serum albumin[22] just as readily as to Aβ and α-synuclein.[23] A recent paper of ours also supports this view, as we characterized by saturation transfer difference (STD) NMR spectroscopy the binding of EGCG and other catechins to Aβ, PrP106-126, and AT3 oligomers.[24] All these data suggest that EGCG targets the only feature shared by the diverse proteins, that is, the polypeptide main chain.

Another well-studied class of natural compounds are tetracyclines, bacteriostatic agents with anti-inflammatory and remarkable neuroprotective properties. Major biological effects of tetracyclines are the inhibition of microglial activation, the attenuation of apoptosis, and the suppression of the production of reactive oxygen species.[25] These mechanisms are involved in the pathogenesis of several neurodegenerative diseases. Furthermore, numerous studies have demonstrated that such compounds are able to prevent fibrillogenesis of prion proteins (PrPs),[26] transthyretin,[27] α-synuclein,[28] β2-microglobulin,[29] and Aβ,[29,30] and, in most of these cases, to dissolve mature fibrils. In particular, it has been established that fibrillogenesis inhibition is a result of non-specific interactions with the different proteins. In this respect, by combining NMR spectroscopy, atomic force microscopy (AFM), FTIR spectroscopy and surface plasmon resonance (SPR) spectroscopy, we showed that co-incubation of tetracycline with Aβ oligomers leads to the formation of colloidal particles that specifically sequester oligomers, thus preventing the progression of the amyloid cascade.[31]

In a previous work, we have demonstrated that EGCG affects the AT3 aggregation pathway by a mechanism similar to that reported for the other mentioned amyloid proteins. In fact, EGCG is able to interfere with the early steps of AT3 aggregation and leads to the formation of off-pathway, non-amyloid, SDS-stable final aggregates. In contrast, tetracycline does not produce major alterations in the structural features of the aggregation intermediates but substantially increases their solubility. Nevertheless, both compounds reduce the toxicity of protein aggregates, as confirmed by their beneficial in vivo effects by using the transgenic *Caenorhabditis elegans* SCA3 model.[13]

Here, we report NMR investigations aimed at providing insight into the mode of interaction of these compounds with the JD, the sole structured part of AT3. For this purpose, we employed both ligand-based and receptor-based NMR methods.[32] We have demonstrated, by using protein solubility assays and FTIR spectroscopy, that the mechanism by which both compounds, EGCG and tetracycline, affect JD aggregation is essentially the same as that observed in the case of expanded AT3.[13] These results further demonstrate the direct involvement of the JD in full-length AT3 fibrillation. By STD NMR experiments we have clearly shown that EGCG is able to bind both the monomeric and the oligomeric JD form, whereas tetracycline can only interact with the oligomeric one. These results strongly support the hypothesis that the capability of EGCG of interfering with the early steps of AT3 aggregation and redirect the process towards a different pathway is due to its ability to bind the monomeric JD. This could account for the different action mechanisms of the two compounds.

Results and Discussion

EGCG and tetracycline differently affect JD aggregation

In a previous work, we demonstrated that EGCG and tetracycline differently modulate the aggregation pathway of an expanded AT3 variant,[13] the former generating SDS-resistant, β-sheet-poor, soluble aggregates, the latter giving rise to aggregated species resembling those arising in the absence of any compound, but substantially more soluble. To further elucidate the mechanism of action of the two compounds, we have examined whether they exert the same effect on JD aggregation, that is, aggregation of the structured N-terminal protein domain. The rationale of our approach relies upon the well-established notion that the aggregation process of full-length AT3, irrespective of the polyQ size, starts with JD misfolding and aggregation, which triggers the earliest steps of expanded AT3 fibrillation.[10,11] Thus, quite plausibly, any treatment affecting or preventing JD aggregation would also affect or prevent the process at the level of full-length AT3.

A His-tagged JD was purified by affinity chromatography and the monomeric form was isolated by size-exclusion chromatography (Figure S1 in the Supporting Information). The protein was then incubated at 37 °C in the presence or the absence of either compound at molar ratios of protein/drug of 1:5. Aliquots were taken at different incubation times and the soluble fraction was isolated as the supernatant from a centrifugation at 14000 *g*. The SDS-soluble protein fraction was quantified by sodium dodecyl sulfate polyacrylamide gel electrophoresis (SDS-PAGE) of the supernatants and subsequent densito-

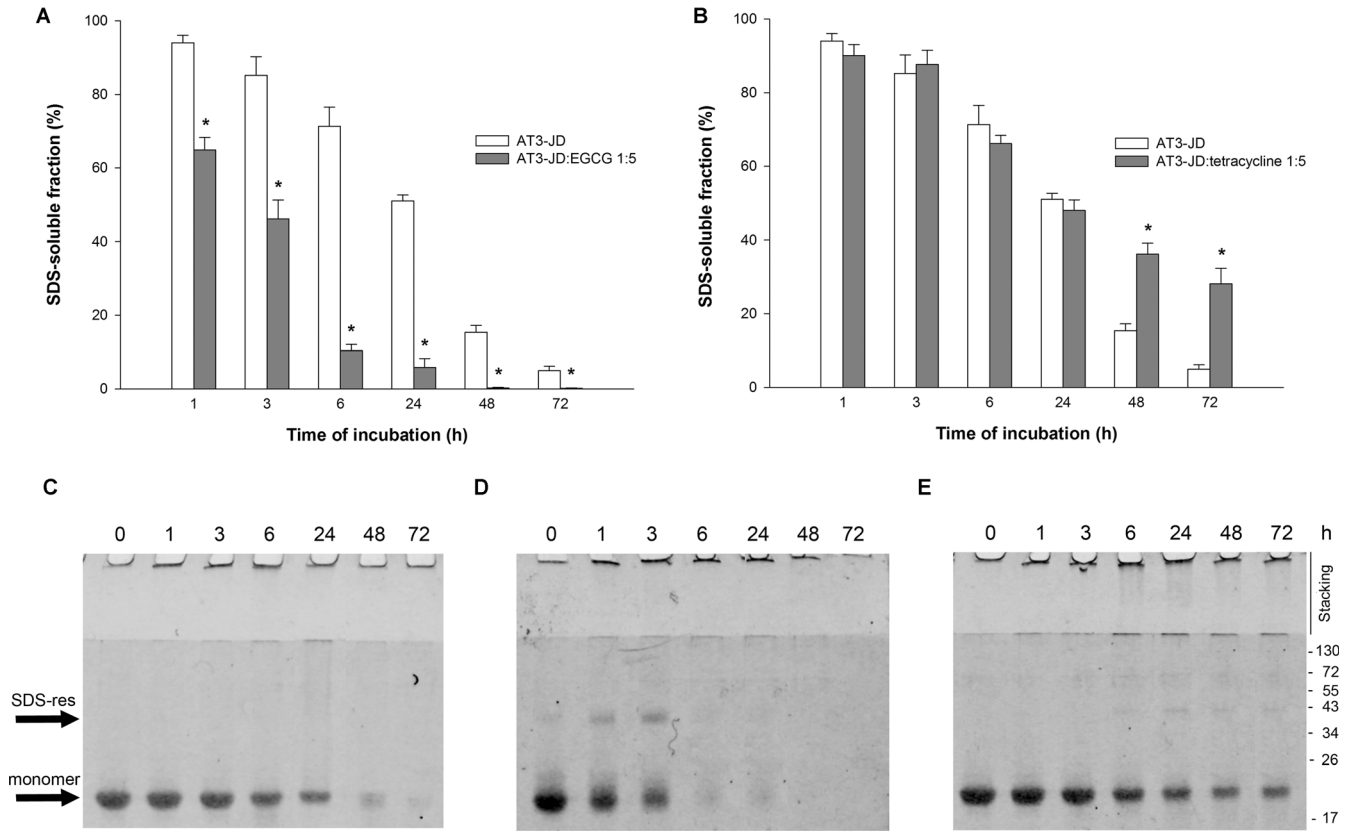

Figure 2. SDS-soluble protein fraction analysis of the JD incubated with EGCG or tetracycline. A 150 μM solution of JD was incubated at 37 °C in the presence or absence of: A) EGCG, or B) tetracycline. The amount of SDS-soluble protein was quantified by centrifuging the incubation mixtures, subjecting the supernatants to SDS-PAGE, and to subsequent densitometric analysis. Signals were normalized at zero-time protein content. Error bars represent standard errors and are derived from at least three independent experiments. * = $P < 0.01$. SDS-PAGE (16%) of the soluble protein fraction of: C) JD, D) JD/EGCG 1:5, and E) JD/tetracycline 1:5. The gels were stained with IRDye blue protein stain (LiCor). The monomeric and the soluble, aggregated, SDS-resistant species are indicated by arrows.

metric analyses. Starting from the earliest incubation time (i.e., 1 h), EGCG treatment resulted in a significant reduction in the SDS-soluble amount of the protein (Figures 2A, C and D). Based on previous work, EGCG may undergo structural changes such as epimerization and dimerization.[33] This prompted us to check its stability. Under our working conditions, the molecule proved to be completely stable, as assessed by ^{1}H NMR spectroscopy, over a time span of 72 h (Figure S2 in the Supporting Information).

In contrast, tetracycline significantly retarded SDS-soluble species disappearance, in particular at the longest incubation times (Figures 2B, C, and E). Size exclusion chromatography (SEC) analyses of the incubation mixtures showed that in the control sample (i.e., JD alone, Figure 3A), higher molecular weight species appeared in the void volume starting from 6 h of incubation. Their estimated molecular mass is 300 kDa or higher. Scanty, if any, accumulation of intermediate forms between the void volume and the monomeric protein was observed. EGCG treatment (Figure 3B) resulted in a much faster disappearance of the monomeric form and accumulation of aggregates. This fits well with the aggregation pattern determined by using SDS-PAGE (Figures 2A and D). In contrast, tetracycline treatment (Figure 3C) did not appreciably alter the JD aggregation pattern as detected by using SEC, which apparently contrasts with our SDS-PAGE results, whereby a much larger accumulation of SDS-soluble species was detected at later times.

One possible explanation might be that there are SDS-soluble aggregated species, which can only be detected by SEC analysis, as already observed in the case of full-length, expanded AT3.[13]. The much higher intensity of the void-volume peak detected in the presence of either compounds, as compared to the control sample, quite likely results from a tight protein–drug interaction, as supported by our observations (data not shown).

EGCG, but not tetracycline, strongly affects the structural features of the aggregation intermediates, as shown by FTIR spectroscopy

The effects of EGCG and tetracycline on the JD misfolding and aggregation were also studied by FTIR spectroscopy in the attenuated total reflection (ATR) mode. The ATR/FTIR absorption spectrum of freshly purified JD is reported in Figure 4A in the amide I band, mainly due to the C=O stretching vibrations of the peptide bond, which is particularly sensitive to protein secondary structures.[34] To disclose the different amide I components, we calculated the second derivative spectrum, whose

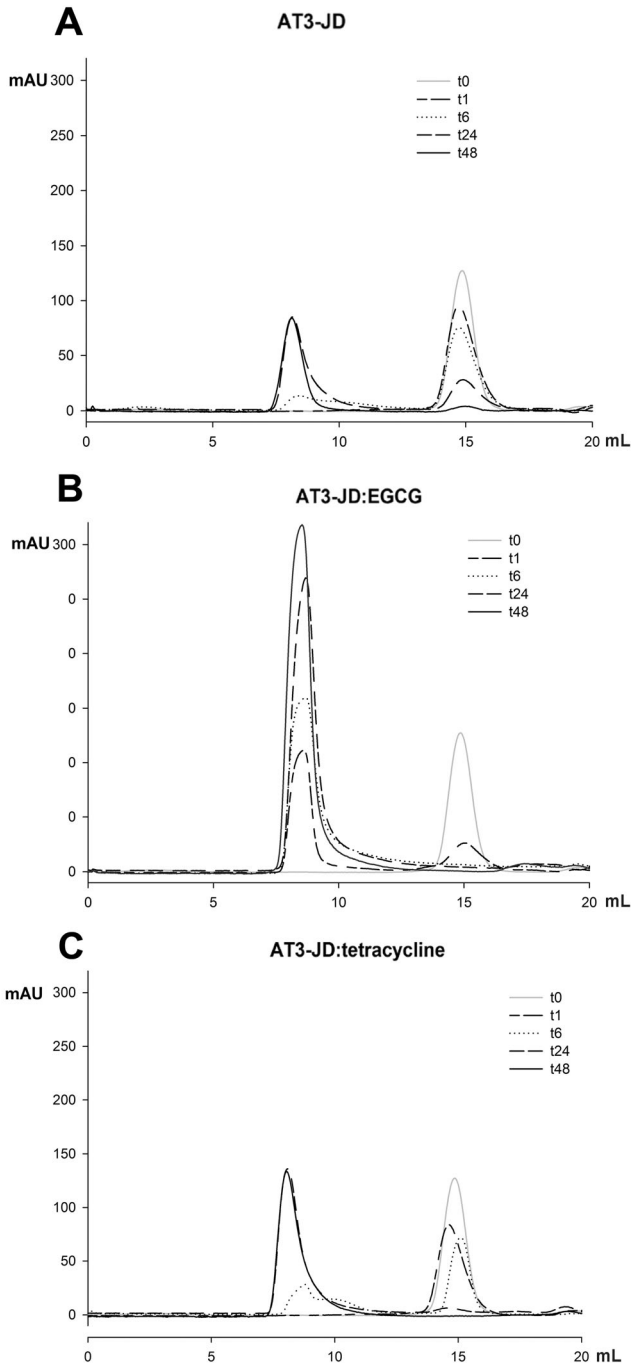

Figure 3. SEC profiles of JD incubated with EGCG or tetracycline. An amount of 500 μg of: A) JD, B) JD/EGCG 1:5, and C) JD/tetracycline 1:5 was loaded onto a Superose 12 10:300 GL column equilibrated in phosphate buffered saline solution after the indicated incubation times.

minima correspond to the absorption maxima.[35] In agreement with previous FTIR characterization of the JD,[12,36] the second derivative spectrum of the native protein (Figure 4B) displayed a major component at approximately $\tilde{\nu}=1635\ cm^{-1}$ that, along with the component at around $\tilde{\nu}=1690\ cm^{-1}$, can be assigned to the native intramolecular β-sheet structures. The component at about $\tilde{\nu}=1657\ cm^{-1}$ occurs in the spectral region of α-helical and random coil structures. During incubation at 37 °C in PBS solution, the amide I peaks of the native protein decreased in intensity and two new components appeared in the spectra at approximately $\tilde{\nu}=1693$ and $1623\ cm^{-1}$ (Figure 4B), which were assigned to the formation of intermolecular β-sheet structures in the protein aggregates.[12] A different behavior was observed in the presence of EGCG (JD/compound 1:5) in comparison with JD alone. Indeed, the second derivative components of the native protein decreased in intensity immediately after EGCG addition, and the peak at about $\tilde{\nu}=1635\ cm^{-1}$ appeared to be downshifted to approximately $\tilde{\nu}=1630\ cm^{-1}$, in the typical spectral region of intermolecular β-sheet structures of protein aggregates (Figure 4C). Very similar spectral changes were previously observed for the full-length expanded AT3 in the presence of EGCG.[13] The presence of an almost constant peak at about $\tilde{\nu}=1630\ cm^{-1}$ suggests that EGCG is able to redirect JD aggregation from the fibril-formation process to off-pathway aggregates. JD second derivative spectra collected at different incubation times in the presence of tetracycline at a JD/compound molar ratio of 1:5 (Figure 4D) indicate that tetracycline does not prevent JD misfolding and aggregation.

However, the final aggregates obtained in the presence of this compound displayed a minor reduction in intensity of the intermolecular β-sheet component, which also occurred at slightly higher wavenumbers compared with the JD alone as shown in Figure 4E, where the second derivative spectra of the pellets obtained after 312 h of protein incubation at 37 °C are reported. In contrast, pellets obtained after incubation with EGCG confirmed the aforementioned downshift to approximately $\tilde{\nu}=1630\ cm^{-1}$, which is indicative of an off-pathway aggregation mode. The time courses of the intensities of native and intermolecular β-sheet structures in the JD aggregates are reported in Figure 4F. Noteworthy, under our conditions, JD misfolding and aggregation at 37 °C in the presence of EGCG was almost completed after an incubation period of 1–2 h, whereas it took about 48 h in the presence of tetracycline, the latter being a pattern essentially indistinguishable from that of the control sample. These results suggest that, unlike tetracycline, EGCG binds to the native JD, leading to the formation of misfolded, aggregation-prone intermediates that are off-pathway of fibrillogenesis.

NMR spectroscopy highlights different interaction modes of EGCG and tetracycline with the JD

Recently, we have extensively exploited STD NMR spectroscopy[37–40] to characterize the binding of several natural[24,31,41,42] and synthetic ligands[43–47] to amyloid oligomers, thus demonstrating the reliability and versatility of this technique. Moreover, Melacini and co-workers validated STD NMR methods in characterizing the amyloid oligomer interaction with soluble proteins (in particular Aβ peptide oligomers)[48,49] and in also mapping peptide early self-association events.[50] In general, when an STD NMR experiment is acquired on a mixture containing the target protein and a potential ligand, the detection of NMR signals of the test molecule in the STD spectra is a clear-cut evidence of an interaction. Here, we have employed STD NMR experiments to investigate the nature of the interac-

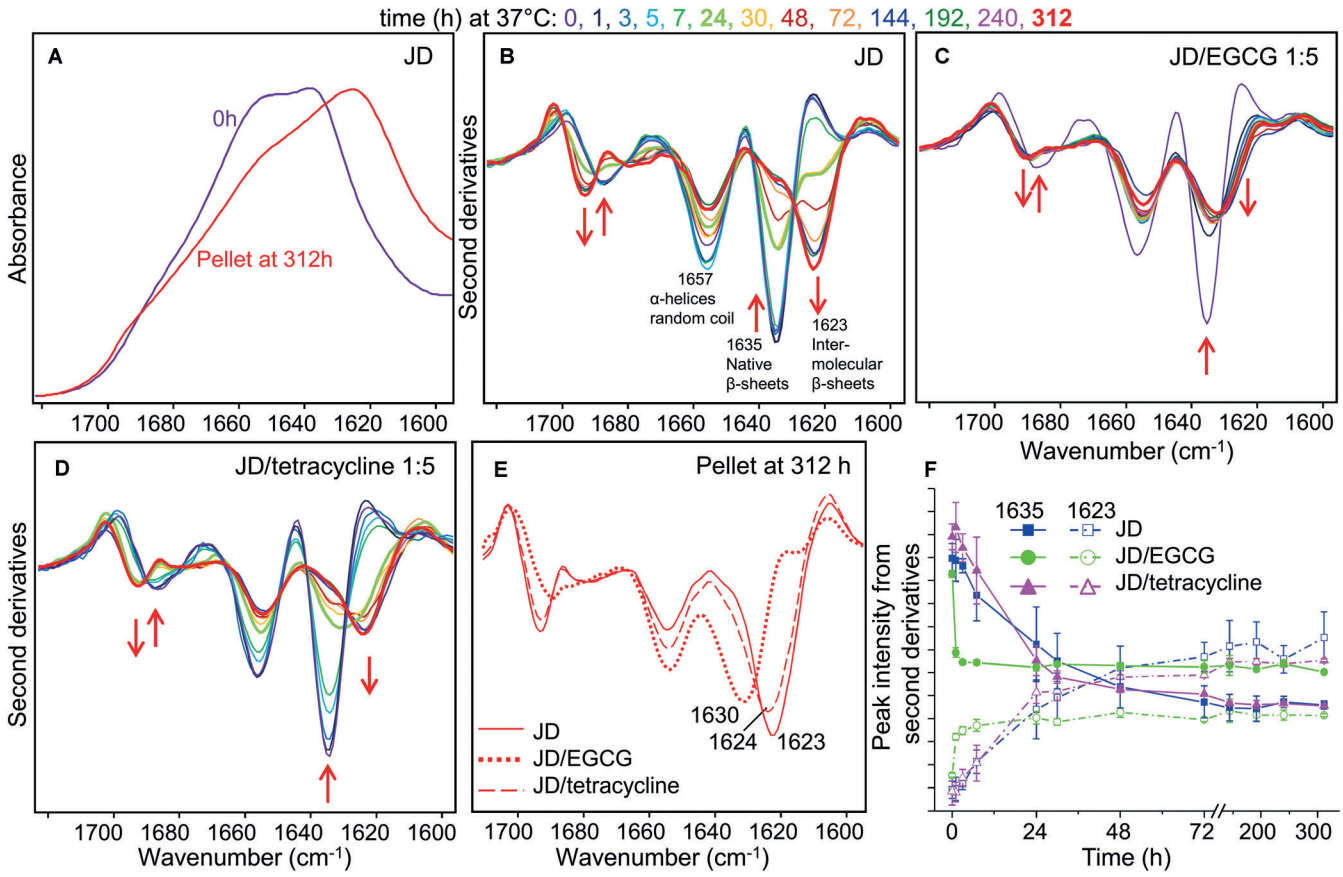

Figure 4. JD misfolding and aggregation studied by using FTIR spectroscopy. A) ATR/FTIR absorption spectra of freshly purified JD and of the pellet collected after incubation of the protein at 37 °C for 312 h. Spectra are reported in the amide I spectral region. B) Second derivatives of the absorption spectra of the JD (150 μM) collected at different incubation times at 37 °C. The assignment of the main components to protein secondary structures are reported. Arrows point to the spectral changes occurring at increasing incubation time. C) Second derivatives of the absorption spectra of 150 μM JD incubated in the presence of 750 μM EGCG (i.e., JD/EGCG 1:5) and otherwise under the conditions reported for panel B. D) Second derivatives of the absorption spectra of 150 μM JD incubated in the presence of 750 μM tetracycline (i.e., JD/tetracycline 1:5) and otherwise under the conditions reported for panel B. E) Second derivative spectra of the pellet collected from a solution of JD incubated in isolation for 312 h at 37 °C, or JD in the presence of EGCG, or of tetracycline. The positions of the main peak, due to β-sheet structures, is indicated. Spectra are shown after normalization at the peak around $\tilde{\nu}=1515$ cm^{-1} of tyrosines to compensate for possible differences in the protein content. F) Time course of the components at $\tilde{\nu}=1635$ and 1623 cm^{-1} (assigned to native JD β-sheets and to intermolecular β-sheet structures of the protein aggregates, respectively) reported for either the JD alone, or incubated in the presence of EGCG or tetracycline. The intensities are taken from the second derivative spectra after normalization of the tyrosine peak approximately appearing at $\tilde{\nu}=1515$ cm^{-1}.

tions of EGCG and tetracycline with both JD monomers and oligomers at the atomic level.

To a solution containing 1.5 mM EGCG or tetracycline in PBS solution, pH 7.2 at 5 °C, an aliquot of monomeric JD was added to a final concentration of 7 μM. Under these conditions, the monomeric state is preserved for at least one day. This is a time suitable for the acquisition of several STD spectra at different saturation times. The same experiments were performed after a pre-incubation period of 5 d at 37 °C of the sole JD. This treatment promotes protein aggregation, with resulting enrichment in JD soluble oligomers, as supported by SEC analysis (Figure S3 in the Supporting Information). STD spectra (Figure 5) unambiguously highlighted a different binding mode by the two compounds. In fact, EGCG resonances appear in both STD spectra depicted in Figure 5A (spectra 2 and 4, recorded in the presence of the JD monomer or the oligomer, respectively), whereas the tetracycline signals are only detected in the STD spectrum recorded in the presence of protein oligomers (Figure 5B, spectrum 4). Thus, the sole EGCG is capable of interacting with the monomeric form, which might, at least in part, account for the different effects of the two compounds in affecting oligomerization.

The binding epitopes identified on either compounds (Figure 6; Figures S4 and S5 in the Supporting Information for the corresponding STD build-up curves) indicate that the whole ligand structure is involved in the receptor recognition process, which is in agreement with previous findings concerning EGCG interaction with AT3Q55 oligomers[24] and tetracycline binding to Aβ oligomers.[31]

In this latter case, we reported in particular the formation of supramolecular colloidal particles presenting a disordered and non-homogeneous internal structure that justifies the absence of a specific ligand binding epitope. We hypothesize the formation of similar supramolecular complexes also in the presence of JD oligomers.

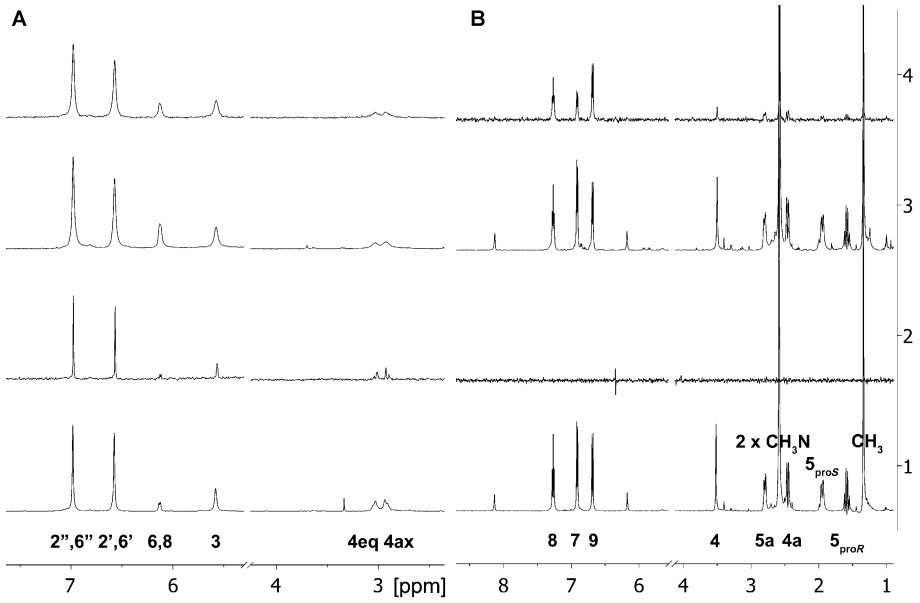

Figure 5. STD NMR characterization of EGCG and tetracycline binding to the JD monomer and oligomers. A) 1) ^{1}H NMR spectrum of a mixture containing JD (7 μM) immediately after purification and 1.5 mM EGCG. 2) STD NMR spectrum of the same mixture investigated in spectrum 1 at a saturation time of 3 s. 3) ^{1}H NMR spectrum of a mixture containing JD (7 μM) five days after purification and 1.5 mM EGCG. 4) STD NMR spectrum of the same mixture investigated in spectrum 3 at a saturation time of 3 s. B) 1) ^{1}H NMR spectrum of a mixture containing JD (7 μM) immediately after purification and 1.5 mM tetracycline. 2) STD NMR spectrum of the same mixture investigated in spectrum 1 at a saturation time of 3 s. 3) ^{1}H NMR spectrum of a mixture containing JD (7 μM) five days after purification and 1.5 mM tetracycline. 4) STD NMR spectrum of the same mixture investigated in spectrum 3 at a saturation time of 3 s. All samples were dissolved in PBS solution, pH 7.2, 5 °C. The spectrometer frequency was 600 MHz. The EGCG H2 signal is overlapped by water resonance. Ligand proton assignment is reported under spectra A1 for EGCG and B1 for tetracycline. All the spectra were recorded at 600 MHz.

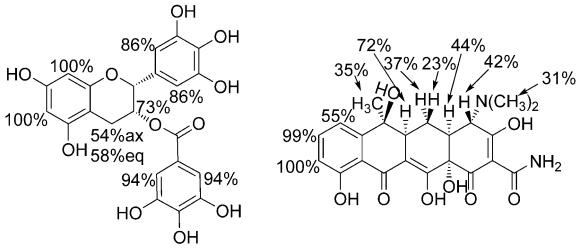

Figure 6. Binding epitopes of EGCG and tetracycline calculated for the interaction with the JD oligomers. In each case, the largest absolute STD effect has been scaled to 100%. The EGCG H2 signal is overlapped by water resonance and thus its STD effect was not calculated.

To provide a complementary insight into the nature of the EGCG interaction with the JD monomers, titration of the ^{15}N-labelled protein with increasing ligand concentrations was performed, and the changes in the protein NMR fingerprint were monitored by acquisition of ^{15}N-SOFAST-HMQC spectra (Figure 7).[51]

First, a SOFAST-HMQC spectrum was acquired on a sample containing 0.3 mM ^{15}N-labelled JD dissolved in PBS solution, pH 6.5 at 25 °C, to verify the match with the backbone amide assignments previously published.[52] Then, the protein was titrated with EGCG (JD/compounds ratios 1:0.5, 1:1, 1:2, 1:3, and 1:4) and the corresponding SOFAST-HMQC spectra were collected (Figure 7). The most significant variation observed is the intensity of the protein cross-peaks, which decreased at each step of titration. This decay correlated with the appearance of a white pellet at the bottom of the NMR tube, occurring after each addition of the ligand, diagnostic of the precipitation of a certain amount of sample. This suggests that the main effect induced by EGCG probably consists in a conformational change of the JD, as already observed by FTIR spectroscopy (Figure 4), which, in turn, promotes fast protein aggregation and precipitation.

The protein sample stability over time in the absence of EGCG was assessed by comparing the SOFAST-HMQC spectra of the JD recorded immediately after purification (Figure 7 A) and after an incubation period of 20 h (which is longer than a full titration experiment) at 25 °C (Figure 7 F). In particular, the protein sample was split into two aliquots, one being employed for the titration experiments (Figures 7 A–E), the other being incubated at 25 °C in the absence of EGCG (Figure 7 F). The spectra given in Figures 7 A and F are identical, supporting the stability of the protein under these experimental conditions.

Thus, protein precipitation is a direct consequence of EGCG addition to the JD sample.

From the comparison of spectra A and C in Figure 7 we derived that, for a protein/ligand molar ratio of 1:1, the amino acid residues most affected by signal broadening are those colored blue in Figure 7 G. They map to the six-stranded antiparallel β-sheet constituting the "core" of the C-terminal subdomain of the JD. Thus, we can infer that the EGCG-induced processes of misfolding and self-aggregation of the JD start in this structural region.

Also, small chemical shift deviations (CSDs) were observed, mainly assigned to residues belonging to the α-helical hairpin moiety (Figure 7 H, pink color). This is a structural motif endowed with high conformational flexibility, likely playing a key role in molecular-recognition and interaction/aggregation processes.[53,54]

Notably, even at high JD/compound ratios and after significant protein precipitation, the ligand resonances were not visible in the ^{1}H NMR spectra of the mixture (Figure S6 in the Supporting Information). This suggests that the stoichiometry of the JD/compound complex should be higher than 1:1 and that at least a part of the ligand precipitates together with the protein aggregates.

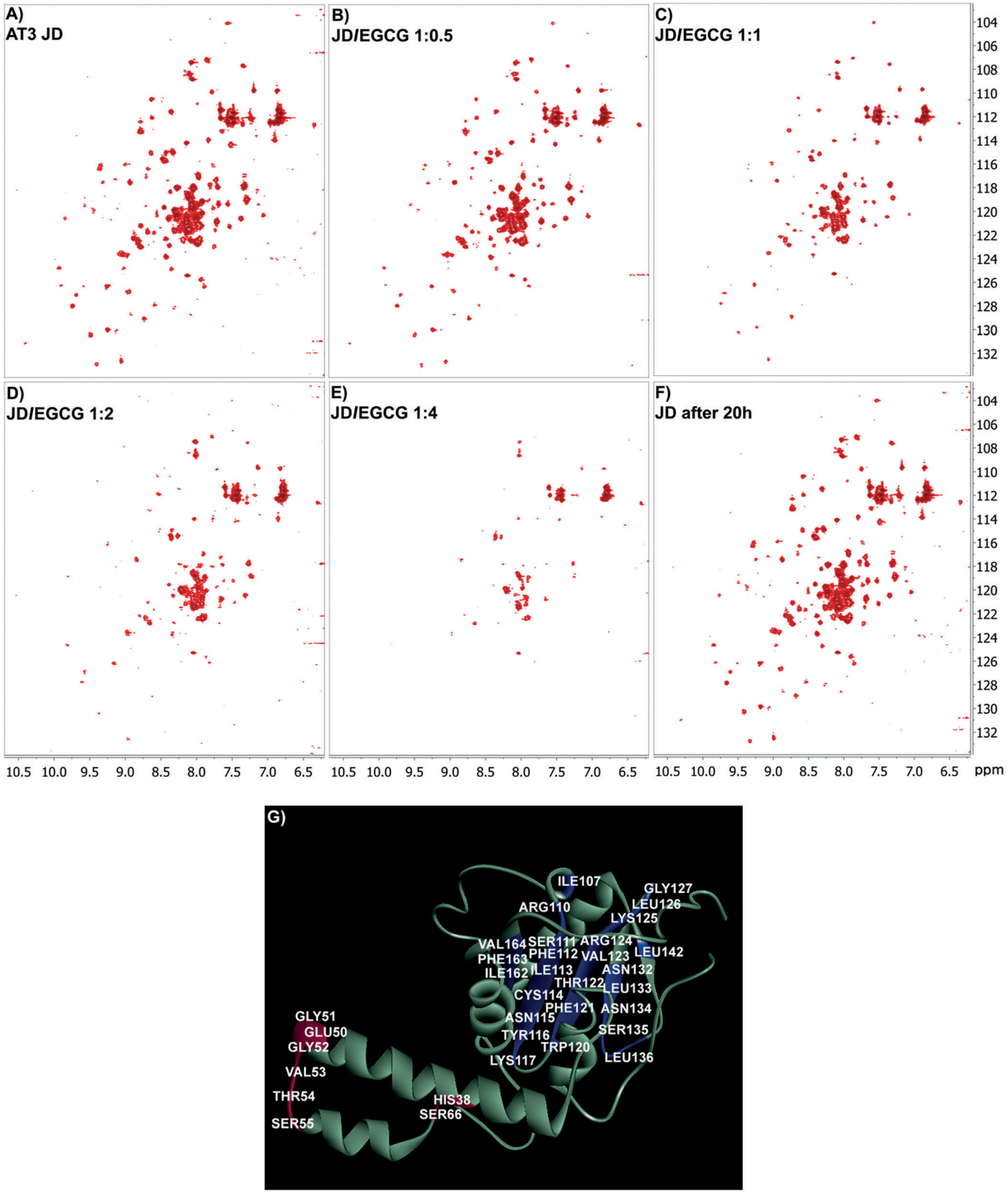

Figure 7. ^{15}N-SOFAST-HMQC titration experiments for the characterization of the EGCG interaction with the JD monomer. The ^{15}N-SOFAST-HMQC spectra were recorded in a solution containing: A) 0.3 mM ^{15}N-JD in PBS solution, pH 6.5 at 25 °C; B) 0.3 mM ^{15}N-JD and 0.15 mM EGCG in PBS solution, pH 6.5 at 25 °C; C) 0.3 mM ^{15}N-JD and 0.3 mM EGCG in PBS solution, pH 6.5 at 25 °C; D) 0.3 mM ^{15}N-JD and 0.6 mM EGCG in PBS solution, pH 6.5 at 25 °C; E) 0.3 mM ^{15}N-JD and 1.2 mM EGCG in PBS solution, pH 6.5 at 25 °C, F) 0.3 mM ^{15}N-JD in PBS solution, pH 6.5, after an incubation period of 20 h at 25 °C. All the spectra were recorded at 600 MHz. G) Residues affected by either signal broadening (blue) or chemical shift perturbation (pink) mapped on the structure of the monomeric JD (PDB ID: 1ZYB).

This is also supported by the dramatic reduction in the diffusion coefficient of EGCG when co-incubated with JD in large stoichiometric excess to JD (JD/EGCG 1:30), as measured by NMR diffusion-ordered spectroscopy (DOSY). The diffusion coefficient of EGCG in the free state (1.5 mM, PBS solution, pH 7.4, 25 °C) was 4.98 m^2s^{-1}, whereas after addition of 50 μM JD, it dropped to 1.96 m^2s^{-1} (reduction of 61%), which supports the existence of an equilibrium free/bound state of the ligand molecules. In the ^{1}H NMR spectra recorded on the same sample prepared for the DOSY acquisition, the EGCG resonances were visible only because of the large ligand stoichiometric excess.

SPR provides evidence of weak JD–EGCG interaction

We performed SPR analyses to determine the binding affinity of the JD–EGCG and JD–tetracycline complexes. In particular, we studied the real time association and dissociation of EGCG or tetracycline to/from JD (Figures 8A and B) coupled directly to the sensor chip CM5 by monitoring the binding and release of EGCG or tetracycline to and from the chip.

In the case of EGCG, the experiments provided evidence of compound binding to the JD. A good fitting was obtained by using the Langmuir 1:1 and BIA evaluation 4.1 software (BIAcore). As the presence of multiple binding sites for EGCG would yield an undistinguishable curve, the K_D value reported in the caption of Figure 8 should be regarded as an apparent one.

No interaction was determined by using tetracycline as an analyte (Figure 8C), which is suggestive of a much lower affinity toward the monomer compared to EGCG, which is in accordance with the NMR data (Figure 5).

Conclusion

In a previous work, we investigated the capability of EGCG and tetracycline to contrast amyloid aggregation and toxicity of full-length expanded variants of AT3.[13] We observed a significant protective effect by both compounds, but also demonstrated substantially different mechanisms of action. Actually, in the presence of EGCG, off-pathway, SDS-resistant soluble aggregates arose, whereas tetracycline did not produce major alterations in the structural features of the aggregates compared with the control, but substantially increased their solubility.

We have thus undertaken the present work to provide insight into how either compound precisely interact with AT3. To this end, we have taken advantage of NMR spectroscopy to identify the individual moieties of the protein and compounds involved in the interaction. However, we have examined their effects on the aggregation of the sole N-terminal JD, as the C-terminal disordered domain would severely hinder NMR measurements.

Our results show that both EGCG and tetracycline affect JD aggregation in a fashion qualitatively similar to that they exert on the full-length, expanded AT3. Most notably, NMR experiments have enabled us to also identify the individual binding epitopes on either compound, which show that the whole ligand structure participates in the protein binding. This points to a nonspecific interaction mode, as also supported by the K_D values assessed by SPR analysis. Not less important, we have also shown that EGCG is able to bind both the monomeric and the oligomeric form of the JD, whereas tetracycline only interacts with the oligomeric one. A possible concern regarding the effects of the two compounds assayed is that they might sequester functional AT3 with a resulting loss of function. However, this should not result in any detrimental effect, as previous work showed that knock-out mice were viable and fertile and did not present a reduced life span.[55]

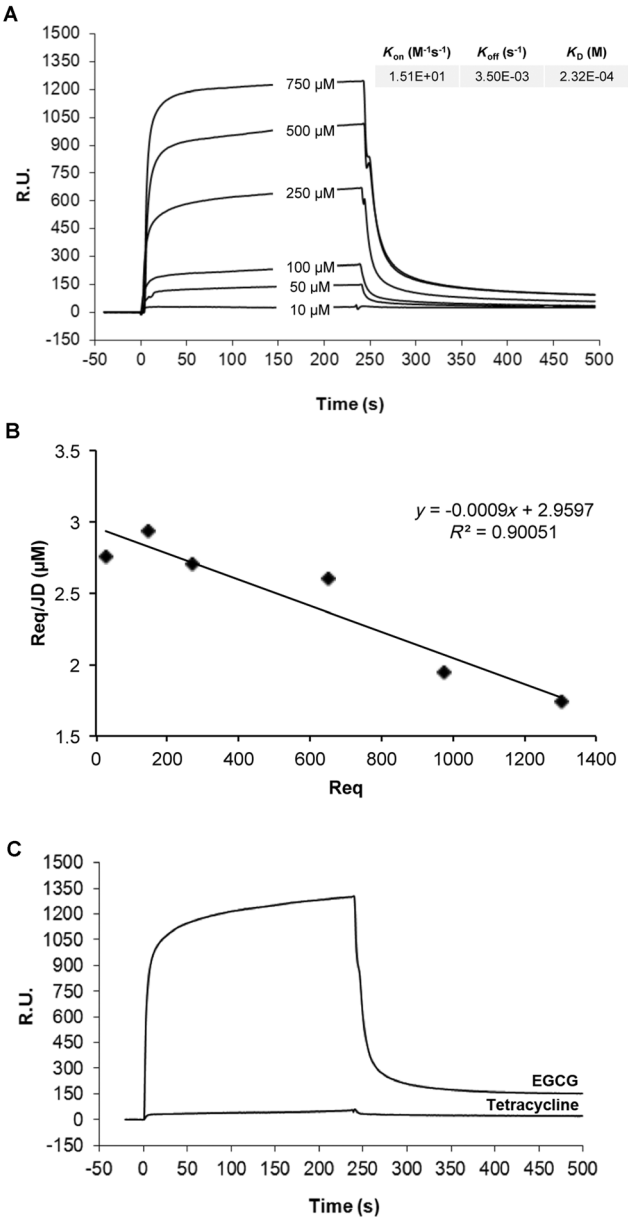

Figure 8. Association/dissociation kinetics for the binding between JD and EGCG. A) JD was immobilized on the sensor chip and the indicated concentrations of EGCG were flowed onto the chip surface. B) The R_{eq} values obtained for each given EGCG concentration were used to generate the Scatchard plot. C) Overlay of the BIAcore sensograms showing the different binding capacity of EGCG and tetracycline (injected at a concentration of 750 μM) for the JD, immobilized on the surface of the sensor chip.

In conclusion, our results suggest that the JD in isolation is a suitable model for assessing the effect of potential antiamyloid agents on AT3, which should significantly speed up research designed for this purpose. This work also provides a more in-depth understanding of the interaction mode between AT3 and the compounds under investigation, which might provide hints to rationally design more effective variants thereof.

Experimental Section

JD purification

The JD-encoding gene was cloned in a pET21-a vector and the protein was expressed in *Escherichia coli* BL21 Tuner (DE3) pLacI (*E. coli* B F^- ompT hsdSB (rB^- mB^-) gal dcm lacY1(DE3) pLacI (CamR); Novagen, Germany) as a His-tagged protein. Cells were grown at 37 °C in LB low salt-ampicillin medium, induced with 0.2 mM isopropylthio-β-D-galactoside (IPTG) at OD_{600} 0.8 for 2 h at 30 °C. Protein purification was performed as previously described for the expanded form.[13] To express the ^{15}N-labeled JD, cells were grown at 37 °C in 2 L of LB low salt-ampicillin in ^{15}N-free medium. At OD_{600} 0.7, the cells were centrifuged for 30 min at 5000 *g*. The pelleted cells were resuspended in isotopically labeled minimal medium (3 g L^{-1} KH_2PO_4, 6 g L^{-1} $Na_2HPO_4{\cdot}7H_2O$, 0.12 g L^{-1} $MgSO_4$, 0.2 g L^{-1} NaCl, 1 g L^{-1} $^{15}NH_4Cl$, 0.4% glucose), then incubated to allow the recovery of growth and clearance of unlabeled metabolites. After 1 h, protein expression was induced with 1 mM IPTG for 2 h at 30 °C.[56] Purification of the labeled protein was performed according to the same protocol as for the unlabeled protein.

SDS-PAGE and densitometry analysis of the soluble protein fraction

The purified JD (150 μM) was incubated at 37 °C in PBS solution in the presence or absence of EGCG or tetracycline (Sigma–Aldrich, USA) at a protein/compound molar ratio of 1:5. JD aliquots at different times of incubation (0, 1, 3, 6, 24, 48, and 72 h) were centrifuged at 14000 *g* for 15 min and 3 μL of the supernatants were subjected to SDS-PAGE. The gels were stained with IRDye Blue Protein Stain (LiCor, USA), scanned at 700 nm with the Odyssey Fc System (LiCor) and analyzed with the Image Studio software (LiCor).

SEC analysis

The purified JD (150 μM) was incubated at 37 °C in PBS solution in the presence or absence of EGCG or tetracycline at a protein/compound molar ratio of 1:5. Aliquots of the protein samples (500 μg) were withdrawn at different times of incubation (0, 1, 6, 24, and 48 h) and loaded onto a Superose 12 10:300 GL gel filtration column (GE Healthcare, Life Sciences, UK), pre-equilibrated with PBS solution (25 mM potassium phosphate, pH 7.2, 150 mM NaCl), and eluted at a flow rate of 0.5 mL min^{-1}.

Fourier transform infrared (FTIR) spectroscopy

FTIR analyses were performed following the experimental procedures already optimized and described in previous FTIR characterizations of JD[12, 36] and of expanded AT3.[12, 13] In particular, a sample (600 μL) of the purified JD (150 μM in PBS solution) was incubated in the test tube at 37 °C in the presence or absence of EGCG or tetracycline at a protein/compound molar ratio of 1:5. An aliquot (3 μL) was taken at different times of incubation and deposited on the diamond element of the device for measurements in the attenuated total reflection (ATR) mode. The Golden Gate (Specac, USA) device with a single reflection diamond crystal was employed. The FTIR spectrum was collected after solvent evaporation, which took place in about 1 min. The formation of a semi-dry film was expected following this procedure.[57] ATR/FTIR spectra were collected by using a Varian 670-IR spectrometer (Varian Australia Pty Ltd, Mulgrave VIC, Australia) equipped with a nitrogen-cooled mercury cadmium telluride detector under the following conditions: 2 cm^{-1} spectral resolution, 25 kHz scan speed, 1000 scans co-addition, and triangular apodization. The ATR/FTIR spectra of a PBS solution and of the two compounds at a concentration of 600 μM in PBS solution were also collected at each incubation time at 37 °C and were subtracted from the protein spectra.[13] Second derivatives of the spectra were obtained, after the smoothing of the measured spectra by the Savitzky–Golay algorithm, by using the software Resolutions Pro (Varian Australia Pty Ltd, Mulgrave VIC, Australia).

NMR spectroscopy

NMR experiments were recorded on a Varian 400 MHz Mercury or a Bruker 600 MHz Avance III spectrometer equipped with a QCI cryo-probe, with a *z*-axis gradient coil. EGCG and tetracycline were dissolved in PBS solution, pH 7.2 and, for ligand–receptor interaction experiments based on ligand observation, an aliquot of the protein solution, dissolved in the same buffer, was added to reach the final concentration required. Conversely, for experiments based on protein observation, small aliquots of a 12 mM EGCG solution in PBS solution, pH 6.5, were added to a sample containing the ^{15}N-labelled JD, with a final maximum dilution of the initial protein concentration of 10%. Sodium azide (0.05%; w/v) was added to the sample to prevent protein degradation by bacteria. Basic sequences were employed for ^1H NMR, STD NMR, ^{15}N-SOFAST-HMQC spectroscopic and diffusion experiments.

Solvent suppression was performed by excitation sculpting. ^1H NMR spectra were acquired with a number of transients ranging from 8 and 256 and 2 s recycle delay. For the STD NMR experiments, a train of Gaussian-shaped pulses each of 50 ms was employed to saturate selectively the protein envelope; the total saturation time of the protein envelope was varied between 3 and 0.15 s, 1024 scans; acquisitions were performed at 5 °C. ^{15}N-SOFAST-HMQC experiments were acquired with a number of transients ranging from 8 and 32, and 640 increments; acquisitions were performed at 25 °C. Diffusion experiments were acquired employing an array of 30 spectra for each experiment (128 scans, with 2 s recycle delay) varying the gradient strength from 3.33 to 19.4 G cm^{-2}. The lengths of and delays between the gradient pulses were optimized depending on the experimental conditions and ranged between 0.002 and 0.005 s and 0.2–0.7 s, respectively; acquisitions were performed at 25 °C. Data fitting and diffusion coefficient determinations were performed by using the software Dosytoolbox (http://personalpages.manchester.ac.uk/staff/mathias.nilsson/software.htm)

Surface plasmon resonance (SPR)

Surface plasmon resonance experiments were carried out with a BIAcore X system (GE Healthcare). JD and AT3Q55 proteins were coupled to a carboxymethylated dextran surface of two different CM5 sensor chips by using amine coupling chemistry at surface densities of 5000 and 4000 resonance units, respectively, by injecting 60 μL of each protein at the concentration of 50 μg mL^{-1} resuspended in 10 mM sodium acetate buffer, pH 4 (flow rate of

5 μL min^{-1}). A reference cell was saturated with 1 M ethanolamine, pH 8.5. Different concentrations of EGCG, diluted in the running buffer (10 mM 4-(2-hydroxyethyl)-1-piperazineethanesulfonic acid (HEPES), pH 7.4, 150 mM NaCl, 3 mM ethylenediaminetetraacetic acid (EDTA), 0.005% v/v Surfactant P20), were tested twice over the surface of sensor chip CM5 for 4 min (40 μL injections at flow rate of 10 μL min^{-1}). Surface regeneration was accomplished by injecting 50 mM NaOH (30 s contact) two or three times. The interaction rate constants were calculated by simultaneous fitting of the binding curves obtained with different concentrations of analyte, by using the BIAevaluation 4.1 software (BIAcore).

Acknowledgements

This work was supported by grants from the Regione Lombardia, Italy (Network-Enabled Drug Design) and the Fondazione Regionale per la Ricerca Biomedica (FRRB). The financial support of the MIUR grant SysBioNet – Italian Roadmap for ESFRI Research Infrastructure – to SYSBIO is also greatly acknowledged. We acknowledge the University of Milano-Bicocca (Fondo Grandi apparecchiature) for the acquisition of the FTIR spectrometer Varian 670-IR and the NMR Bruker Avance III 600 MHz spectrometer.

Keywords: aggregation inhibitors · epigallocatechin-3-gallate · Josephin domain · molecular recognition · tetracyclines

[1] Y. Trottier, Y. Lutz, G. Stevanin, G. Imbert, D. Devys, G. Cancel, F. Saudou, C. Weber, G. David, L. Tora, *Nature* **1995**, *378*, 403 – 406.
[2] Y. Kawaguchi, T. Okamoto, M. Taniwaki, M. Aizawa, M. Inoue, S. Katayama, H. Kawakami, S. Nakamura, M. Nishimura, I. Akiguchi, *Nat. Genet.* **1994**, *8*, 221 – 228.
[3] B. T. Koshy, H. Y. Zoghbi, *Brain Pathol.* **1997**, *7*, 927 – 942.
[4] H. L. Paulson, S. Das, P. B. Crino, M. K. Perez, S. C. Patel, D. Gotsdiner, K. H. Fischbeck, R. N. Pittman, *Ann. Neurol.* **1997**, *41*, 453 – 462.
[5] Q. S. Padiath, A. K. Srivastava, S. Roy, S. Jain, S. K. Brahmachari, *Am. J. Med. Genet. Part B Neuropsychiatr. Genet. Off. Publ. Int. Soc. Psychiatr. Genet.* **2005**, *133B*, 124 – 126.
[6] L. Masino, V. Musi, R. P. Menon, P. Fusi, G. Kelly, T. A. Frenkiel, Y. Trottier, A. Pastore, *FEBS Lett.* **2003**, *549*, 21 – 25.
[7] L. Masino, G. Nicastro, R. P. Menon, F. Dal Piaz, L. Calder, A. Pastore, *J. Mol. Biol.* **2004**, *344*, 1021 – 1035.
[8] M. K. M. Chow, A. M. Ellisdon, L. D. Cabrita, S. P. Bottomley, *Biol. Chem.* **2004**, *279*, 47643 – 47651.
[9] A. M. Ellisdon, B. Thomas, S. P. Bottomley, *J. Biol. Chem.* **2006**, *281*, 16888 – 16896.
[10] A. L. Robertson, S. J. Headey, H. M. Saunders, H. Ecroyd, M. J. Scanlon, J. A. Carver, S. P. Bottomley, *Proc. Natl. Acad. Sci. USA* **2010**, *107*, 10424 – 10429.
[11] L. Masino, G. Nicastro, A. De Simone, L. Calder, J. Molloy, A. Pastore, *Biophys. J.* **2011**, *100*, 2033 – 2042.
[12] A. Natalello, A. M. Frana, A. Relini, A. Apicella, G. Invernizzi, C. Casari, A. Gliozzi, S. M. Doglia, P. Tortora, M. E. Regonesi, *PLoS One* **2011**, *6*, e18789.
[13] M. Bonanomi, A. Natalello, C. Visentin, V. Pastori, A. Penco, G. Cornelli, G. Colombo, M. G. Malabarba, S. M. Doglia, A. Relini, M. E. Regonesi, P. Tortora, *Hum. Mol. Genet.* **2014**, *23*, 6542 – 6552.
[14] J. V. Higdon, B. Frei, *Crit. Rev. Food Sci. Nutr.* **2003**, *43*, 89 – 143.
[15] C. S. Yang, Z. Y. Wang, *J. Natl. Cancer Inst.* **1993**, *85*, 1038 – 1049.
[16] F. Jiang, G. Dusting, *J. Curr. Vasc. Pharmacol.* **2003**, *1*, 135 – 156.
[17] A. Higuchi, K. Yonemitsu, A. Koreeda, S. Tsunenari, *Toxicology* **2003**, *183*, 143 – 149.
[18] K. Rezai-Zadeh, G. W. Arendash, H. Hou, F. Fernandez, M. Jensen, M. Runfeldt, R. D. Shytle, J. Tan, *J. Brain Res.* **2008**, *1214*, 177 – 187.
[19] J. Bieschke, J. Russ, R. P. Friedrich, D. E. Ehrnhoefer, H. Wobst, K. Neugebauer, E. E. Wanker, *Proc. Natl. Acad. Sci. USA* **2010**, *107*, 7710 – 7715.
[20] N. Ferreira, I. Cardoso, M. R. Domingues, R. Vitorino, M. Bastos, G. Bai, M. J. Saraiva, M. R. Almeida, *FEBS Lett.* **2009**, *583*, 3569 – 3576.
[21] D. E. Ehrnhoefer, M. Duennwald, P. Markovic, J. L. Wacker, S. Engemann, M. Roark, J. Legleiter, J. L. Marsh, L. M. Thompson, S. Lindquist, P. J. Muchowski, E. E. Wanker, *Hum. Mol. Genet.* **2006**, *15*, 2743 – 2751.
[22] M. Li, A. E. Hagerman, *J. Agric. Food Chem.* **2014**, *62*, 3768 – 3775.
[23] D. E. Ehrnhoefer, J. Bieschke, A. Boeddrich, M. Herbst, L. Masino, R. Lurz, S. Engemann, A. Pastore, E. E. Wanker, *Nat. Struct. Mol. Biol.* **2008**, *15*, 558 – 566.
[24] E. Sironi, L. Colombo, A. Lompo, M. Messa, M. Bonanomi, M. E. Regonesi, M. Salmona, C. Airoldi, *Chem. Eur. J.* **2014**, *20*, 13793 – 13800.
[25] M. Domercq, C. Matute, *Trends Pharmacol. Sci.* **2004**, *25*, 609 – 612.
[26] G. Forloni, M. Salmona, G. Marcon, F. Tagliavini, *Infect. Disord.: Drug Targets* **2009**, *9*, 23 – 30.
[27] I. Cardoso, M. J. Saraiva, *FASEB J.* **2006**, *20*, 234 – 239.
[28] K. Ono, M. Yamada, *J. Neurochem.* **2006**, *97*, 105 – 115.
[29] S. Giorgetti, S. Raimondi, K. Pagano, A. Relini, M. Bucciantini, A. Corazza, F. Fogolari, L. Codutti, M. Salmona, P. Mangione, L. Colombo, A. De Luigi, R. Porcari, A. Gliozzi, M. Stefani, G. Esposito, V. Bellotti, M. Stoppini, *J. Biol. Chem.* **2011**, *286*, 2121 – 2131.
[30] G. Forloni, L. Colombo, L. Girola, F. Tagliavini, M. Salmona, *FEBS Lett.* **2001**, *487*, 404 – 407.
[31] C. Airoldi, L. Colombo, C. Manzoni, E. Sironi, A. Natalello, S. M. Doglia, G. Forloni, F. Tagliavini, E. Del Favero, L. Cantù, F. Nicotra, M. Salmona, *Org. Biomol. Chem.* **2011**, *9*, 463 – 472.
[32] L. Unione, S. Galante, D. Díaz, F. J. Cañada, J. Jiménez-Barbero, *Med. Chem. Commun.* **2014**, *5*, 1280 – 1289.
[33] S. Sang, M. J. Lee, Z. Hou, C. T. Ho, C. S. Yang, *J. Agric. Food Chem.* **2005**, *53*, 9478 – 9484.
[34] A. Barth, *Biochim. Biophys. Acta Bioenerg.* **2007**, *1767*, 1073 – 1101.
[35] H. Susi, D. M. Byler, *Methods Enzymol.* **1986**, *130*, 290 – 311.
[36] A. Apicella, A. Natalello, A. M. Frana, A. Baserga, C. S. Casari, C. E. Bottani, S. M. Doglia, P. Tortora, M. E. Regonesi, *Biochimie* **2012**, *94*, 1026 – 1031.
[37] M. Mayer, B. Meyer, *Angew. Chem. Int. Ed.* **1999**, *38*, 1784 – 1788; *Angew. Chem.* **1999**, *111*, 1902 – 1906.
[38] R. Caraballo, H. Dong, J. P. Ribeiro, J. Jiménez-Barbero, O. Ramström, *Angew. Chem. Int. Ed.* **2010**, *49*, 589 – 593; *Angew. Chem.* **2010**, *122*, 599 – 603.
[39] a) A. Palmioli, E. Sacco, C. Airoldi, F. Di Nicolantonio, A. D'Urzo, S. Shirasawa, T. Sasazuki, A. Di Domizio, L. De Gioia, E. Martegani, A. Bardelli, F. Peri, M. Vanoni, *Biochem. Biophys. Res. Commun.* **2009**, *386*, 593 – 597; b) C. Airoldi, S. Sommaruga, S. Merlo, P. Sperandeo, L. Cipolla, A. Polissi, F. Nicotra, *Chem. Eur. J.* **2010**, *16*, 1897 – 1902; c) C. Airoldi, S. Sommaruga, S. Merlo, P. Sperandeo, L. Cipolla, A. Polissi, F. Nicotra, *ChemBioChem* **2011**, *12*, 719 – 727.
[40] C. Airoldi, S. Giovannardi, B. La Ferla, J. Jiménez-Barbero, F. Nicotra, *Chem. Eur. J.* **2011**, *17*, 13395 – 13399.
[41] C. Airoldi, E. Sironi, C. Dias, F. Marcelo, A. Martins, A. P. Rauter, F. Nicotra, J. Jimenez-Barbero, *Chem. Asian J.* **2013**, *8*, 596 – 602.
[42] A. R. Jesus, C. Dias, A. M. Matos, R. F. M. deAlmeida, A. S. Viana, F. Marcelo, R. T. Ribeiro, M. P. Macedo, C. Airoldi, F. Nicotra, A. Martins, E. J. Cabrita, J. Jiménez-Barbero, A. P. Rauter, *J. Med. Chem.* **2014**, *57*, 9463 – 9472.
[43] C. Airoldi, C. Zona, E. Sironi, L. Colombo, M. Messa, D. Aurilia, M. Gregori, M. Masserini, M. Salmona, F. Nicotra, B. La Ferla, *J. Biotechnol.* **2011**, *156*, 317 – 324.
[44] C. Airoldi, F. Cardona, E. Sironi, L. Colombo, M. Salmona, A. Silva, F. Nicotra, B. La Ferla, *Chem. Commun.* **2011**, *47*, 10266 – 10268.
[45] C. Airoldi, F. Cardona, E. Sironi, L. Colombo, M. Salmona, I. Cambianica, F. Ornaghi, G. Sancini, F. Nicotra, B. La Ferla, *Pure Appl. Chem.* **2013**, *85*, 1813 – 1823.
[46] S. Merlo, E. Sironi, L. Colombo, F. Cardona, A. M. Martorana, M. Salmona, B. La Ferla, C. Airoldi, *ChemPlusChem* **2014**, *79*, 835 – 843.
[47] C. Airoldi, S. Mourtas, F. Cardona, C. Zona, E. Sironi, G. D'Orazio, E. Markoutsa, F. Nicotra, S. G. Antimisiaris, B. La Ferla, *Eur. J. Med. Chem.* **2014**, *85*, 43 – 50.
[48] J. Milojevic, A. Raditsis, G. Melacini, *Biophys. J.* **2009**, *97*, 2585 – 2594.
[49] J. Milojevic, A. G. Melacini, *Biophys. J.* **2011**, *100*, 183 – 192.

[50] H. Huang, J. Milojevic, G. Melacini, *J. Phys. Chem. B* **2008**, *112*, 5795 – 5802.
[51] P. Schanda, E. Kupce, B. Brutscher, *J. Biomol. NMR* **2005**, *33*, 199 – 211.
[52] G. Nicastro, L. Masino, T. A. Frenkiel, G. Kelly, J. McCormick, R. P. Menon, A. Pastore, *J. Biomol. NMR* **2004**, *30*, 457 – 458.
[53] G. Nicastro, R. P. Menon, L. Masino, P. P. Knowles, N. Q. McDonald, A. Pastore, *Proc. Natl. Acad. Sci. USA* **2005**, *102*, 10493 – 10498.
[54] D. Sanfelice, A. De Simone, A. Cavalli, S. Faggiano, M. Vendruscolo, A. Pastore, *Biophys. J.* **2014**, *107*, 2932 – 2940.
[55] P. M. Switonski, A. Fiszer, K. Kazmierska, M. Kurpisz, W. J. Krzyzosiak, M. Figiel, *Neuromolecular Med.* **2011**, *13*, 54 – 65.
[56] J. Marley, M. Lu, C. Bracken, *J. Biomol. NMR* **2001**, *20*, 71 – 75.
[57] E. Goormaghtigh, V. Raussens, J. M. Ruysschaert, *Biochim. Biophys. Acta Rev. Biomembr.* **1999**, *1422*, 105 – 185.

Received: August 5, 2015
Published online on ■■ ■■, 0000

FULL PAPER

Molecular Recognition

M. Bonanomi, C. Visentin, A. Natalello, M. Spinelli, M. Vanoni, C. Airoldi, M. E. Regonesi,* P. Tortora*

■■ – ■■

How Epigallocatechin-3-gallate and Tetracycline Interact with the Josephin Domain of Ataxin-3 and Alter Its Aggregation Mode

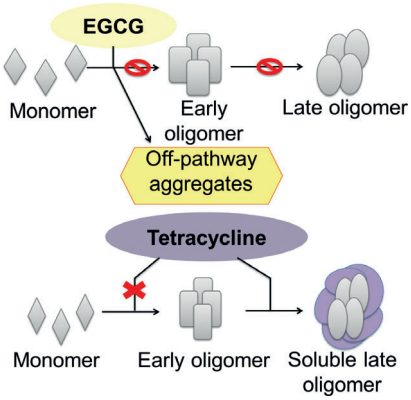

All roads are nontoxic: Epigallocatechin-3-gallate (EGCG) and tetracycline affect the aggregation of the Josephin domain of ataxin-3 in a very different way (see figure).